International Journal of Multiphase Flow 36 (2010) 467–480

Contents lists available at ScienceDirect

International Journal of Multiphase Flow

journal homepage: www.elsevier.com/locate/ijmulflow

Single-beam gamma densitometry measurements of oil–water flow in horizontal and slightly inclined pipes

W.A.S. Kumara, B.M. Halvorsen, M.C. Melaaen *

Telemark University College, PO Box 203, N-3901 Porsgrunn, Norway

ARTICLE INFO

Article history:
Received 7 June 2009
Received in revised form 1 October 2009
Accepted 3 February 2010
Available online 4 March 2010

Keywords:
Gamma densitometry
Water hold-up
Slip ratio
Frictional pressure drop

ABSTRACT

Gamma densitometry is a frequently used non-intrusive method for measuring component volume fractions in multiphase flow systems. The application of a single-beam gamma densitometer to investigate oil–water flow in horizontal and slightly inclined pipes is presented. The experiments are performed in a 15 m long, 56 mm diameter, inclinable stainless steel pipe using Exxsol D60 oil (viscosity 1.64 mPa s, density 790 kg/m^3) and water (viscosity 1.0 mPa s, density 996 kg/m^3) as test fluids. The test pipe inclination is changed in the range from 5° upward to 5° downward. Experimental measurements are reported at three different mixture velocities, 0.25, 0.50 and 1.00 m/s, and the inlet water cut is varied from 0 to 1. The gamma densitometer is composed of radioactive isotope of Am-241 with the emission energy of 59.5 keV, scintillation detector [NaI(Tl)] and signal processing system. The time averaged cross-sectional distributions of oil and water phases are measured by traversing the gamma densitometer along the vertical pipe diameter. Based on water volume fraction measurements, water hold-up and slip ratio are estimated. The total pressure drop over the test section is measured and frictional pressure drop is estimated based on water hold-up measurements. The measurement uncertainties associated with gamma densitometry are also discussed. The measured water hold-up and slip ratio profiles are strongly dependent on pipe inclination. In general, higher water hold-up values are observed in upwardly inclined pipes compared to the horizontal and downwardly inclined pipes. At low mixture velocities, the slip ratio decreases as the water cut increases. The decrease is more significant as the degree of inclination increases. The frictional pressure drop for upward flow is slightly higher than the horizontal flow. In general, there is a marginal difference in frictional pressure drop values for horizontal and downwardly inclined flows.

1. Introduction

The hold-up measurement techniques based on radiation attenuation have been extensively used in multiphase flow applications (Hewitt, 1978; Åbro and Johansen, 1998). In most applications, it is the attenuation of radiation (neutron, X-ray and gamma-ray) that serves as the basis for the measurements. However, gamma densitometry has several advantages compared to the other radiation attenuation methods. The higher penetration capabilities of gamma-rays in comparison to neutron beams make it ideal system for measuring phase fractions in large industrial systems (Chaouki et al., 1997). In addition, it is less expensive compared to the neutron densitometry. The gamma-ray attenuation systems produce mono-energetic rays without intensity fluctuations contrary to X-ray attenuation techniques (Stahl and Rohr, 2004). The gamma-ray densitometry is a non-intrusive technique that does not disturb the flow under investigation. The technique has been widely applied in a variety of multiphase flow systems in chemical and petrochemical processes. Bukur et al. (1996) measured the gas hold-up and flow regime transition in bubble column using gamma-ray attenuation. Eberle et al. (1994) applied a novel theoretical method for optimization of a gamma densitometer to measure area averaged void fraction in gas–liquid flow. The gamma densitometry has also been successfully applied in oil–water flows to measure local phase fractions (Elseth, 2001; Rodriguez and Oliemans, 2006). The MultiPhase Flow Meters (MPFMs) that measure the water, oil and gas flows offer online measurements and better control in order to optimize the production in offshore installations. The component phase fractions in the multiphase flows must be measured in order to estimate mass flow rates. MPFMs should preferably have non-intrusive sensors for several reasons, including the elimination of pressure drop over the instrument, lack of impact on the flow and the elimination of detector corrosion (Åbro and Johansen, 1998). The gamma-ray attenuation technique is one of the most commonly used method for measuring void fractions in modern MPFMs (Thorn et al., 1997).

Chaouki et al. (1997) have written an extensive outline of the existing gamma densitometry methods. The basic design of a gamma-ray densitometer consists of a radioactive source, detector and

* Corresponding author. Tel.: +47 35 57 52 86; fax: +47 35 57 50 02.
E-mail address: Morten.C.Melaaen@hit.no (M.C. Melaaen).

0301-9322/$ - see front matter © 2010 Elsevier Ltd. All rights reserved.
doi:10.1016/j.ijmultiphaseflow.2010.02.003

signal processing system. The "heart" of the instrument is the radioactive source providing gamma radiation at a constant intensity. The gamma radiation passes through the test volume to the detector system. The degree of attenuation experienced by a narrow beam of gamma radiation is a function of the gamma beam photons' energy and the density of the absorbing matter (Blaney and Yeung, 2007). In two-phase flows, this can be calibrated to measure the component fractions in the volume covered by the gamma beam. The measurements of volume fractions are generally dependent on the internal distribution of the components inside the pipeline, i.e. on the flow regime. As the structure of the flow patterns is often unknown or mathematically not exactly describable, the flow pattern dependence is usually neglected in order to calculate volume fractions from gamma-ray attenuation data (Petrick and Swanson, 1958; Spindler et al., 1988; Jiang and Rezkallah, 1993). A higher accuracy in the measurements can be achieved by multi-beam and multi-source methods, because multi-path interrogation enables to calculate the phase fractions of multiphase flow systems without the need to characterize the flow regime. The phase distribution can be reconstructed numerically using discrete attenuation data from each beam location (Stahl and Rohr, 2004).

Wire-mesh sensors are emerging as a phase distribution measurement technique, which can compete with the multi-beam and multi-source radiation attenuation methods. Prasser et al. (1998) described the function and construction of wire-mesh sensors. In addition to the phase distribution measurements, wire-mesh sensors are capable of providing high-speed flow visualization as well as the measurements of bubble size distributions and gas velocity distributions (Prasser, 2008). The method has been extensively applied in gas–liquid flow. However, the technique can also be applied for oil–water flows due to the differences in electrical conductivity of the phases. Nevertheless, these complex systems are more expensive than simple single-beam gamma attenuation methods. Hence, both in industrial and engineering research applications single-beam gamma densitometers are used extensively for phase fraction measurements in multiphase flow systems.

In the present work, single-beam gamma densitometry is used for non-intrusive measurements of local phase distributions in oil–water flows in horizontal and slightly inclined pipes. In the experiments, the vertical interface position is measured by traversing horizontal gamma beams. The water hold-up and slip ratio are calculated based on time averaged gamma densitometry measurements. The total pressure drop over the test section is measured and frictional pressure drop is calculated based on water hold-up measurements. The measurement uncertainties associated with single-beam gamma densitometry are also discussed.

2. Theory

Gamma densitometry exploits the fact that electromagnetic radiation is attenuated as it passes through matter owing to the interaction of its photons with the matter. There are more than ten types of elementary processes of interaction of gamma rays with matter (Fano, 1953). The two main interactions concerning gamma densitometry attenuation are photoelectric and Compton scattering interactions (Sprowll and Phillips, 1980). The photoelectric effect generally predominates at lower radiation energies and higher ordinal numbers of the absorber, whereas the Compton effect is more predominant at higher radiation energies, more than 100 keV (Schlieper et al., 1987). Thus, the photoelectric effect is the main interaction process for Am-241 source with the emission energy of 59.5 keV, in the present experiments.

The capability of material to absorb gamma radiation is characterized by its mass absorption coefficient (μ). The attenuation of mono energetic gamma-radiation in homogeneous material and its resulting exponential loss of intensity is governed by the Beer–Lambert's law, which can be expressed as (Chaouki et al., 1997):

$$I = I_0 \exp(-\rho\mu x) = I_0 \exp(-\kappa x) \tag{1}$$

I_0 is the incident or initial radiation intensity, while I is the intensity of radiation detected after the beam has traveled a distance x through the absorbing material. ρ represents the density of the absorption material. The linear attenuation coefficient (κ) is defined as the product of mass absorption coefficient and the density of absorbing material. The value of the mass absorption coefficient depends on the absorbing material and on the radiation energy. Pan (1996) correlated the linear attenuation coefficient as a function of gamma radiation energies for oil and water, from the data given by Grodstein (1957). In general, the linear attenuation coefficient of water is higher than oil and it is possible to use this difference in attenuation of gamma radiation as an indication to distinguish oil and water phases in a test volume. In the present experiments, Am-241 source with radiation energy of 59.5 keV is used. At this energy level, the difference between the linear attenuation coefficients of water and oil is about 5.0 m^{-1}.

In two-phase oil–water flow measurements, the geometric distribution of the two phases affects the signal conversion method in gamma densitometry. The two extreme configurations are shown by Petrick and Swanson (1958), in which the phases are distributed in layers parallel or perpendicular to the beam. The linear and logarithmic approximations for describing the correlations between the loss of radiation intensity in a test volume and its phase fraction can be derived by considering a square control volume, filled with oil and water as illustrated in Fig. 1. In both cases, the water volume fraction ε_w can be defined as:

$$\varepsilon_w = \frac{x_w}{x_o + x_w} = \frac{x_w}{x} \tag{2}$$

where x_o and x_w are the path lengths of the beam in the oil and water phases, respectively. The attenuation of gamma radiation for the perpendicular distribution as shown in Fig. 1a can be given as:

$$I = I_0 \exp\left[-(\rho_o\mu_o x_o + \rho_w\mu_w x_w)\right] \tag{3}$$

where μ_o and μ_w are the mass absorption coefficients of oil and water, respectively. The oil and water phase densities are represented by ρ_o and ρ_w. Similarly, the parallel distribution as shown in Fig. 1b yields:

$$I = \frac{x_o}{x} I_0 \exp(-\rho_o\mu_o x) + \frac{x_w}{x} I_0 \exp(-\rho_w\mu_w x) \tag{4}$$

The transmitted intensity of purely oil filled test volume is given as:

$$I_0 = I_0 \exp(-\rho_o\mu_o x) \tag{5}$$

The analogous transmitted intensity of the purely water filled test volume can be expressed similarly:

$$I_w = I_0 \exp(-\rho_w\mu_w x) \tag{6}$$

Eqs. (2), (3), (5), and (6) can be combined in order to obtain a logarithmic relation for the water volume fraction in the test volume for perpendicular phase distribution as given below:

$$\varepsilon_w = \frac{\ln(\frac{I}{I_o})}{\ln(\frac{I_w}{I_o})} \tag{7}$$

Similarly, Eqs. (2), (4), (5), and (6) can be combined to yield linear relation for parallel phase distribution as follows:

$$\varepsilon_w = \frac{I - I_o}{I_w - I_o} \tag{8}$$

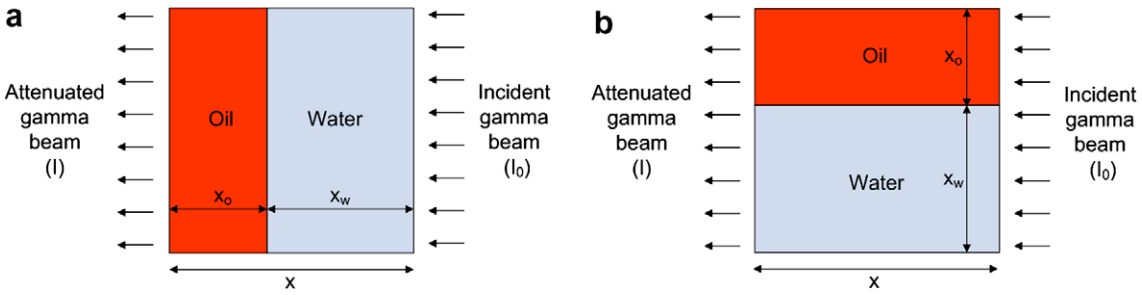

Fig. 1. Attenuation of gamma radiation in a square test volume filled with oil and water: (a) radiation perpendicular to the interface, (b) radiation parallel to the interface.

where I_o and I_w are the calibrated values, i.e. the photon rates measured for single-phase oil and water. In real situation the configuration will lie somewhere in between these two extremes, but the authors tend to favour Eq. (7) (Petrick and Swanson, 1958). Hence, logarithmic approximation is used to estimate water volume fractions throughout this article. These approximations are applicable only in two-phase systems and only when a narrow collimated beam is used in the measurement process (Chaouki et al., 1997). In principle, the water volume fraction profile can be determined to a fine detail by having a source emitting a narrow beam of radiation and an opposing detector scan across the cross-section. This yields a series of chordal averaged volume fraction measurements. The significance of Eqs. (7) and (8) is that the volume fractions determined in this way is independent of I_0 (which depends on the source strength, the distance between the source and detector and the detector efficiency), independent of μ_w and μ_o (which depend on the pressure and temperature) and independent of the attenuation in the pipe wall (Kok et al., 2001).

3. Experimental set-up

The experiments were performed in the multiphase flow facility at Telemark University College, Porsgrunn, Norway. A simplified flow sheet of the experimental rig is shown in Fig. 2, which is described in detail by Kumara et al. (2009a). All experiments are conducted using Exxsol D60 oil and water at room temperature and

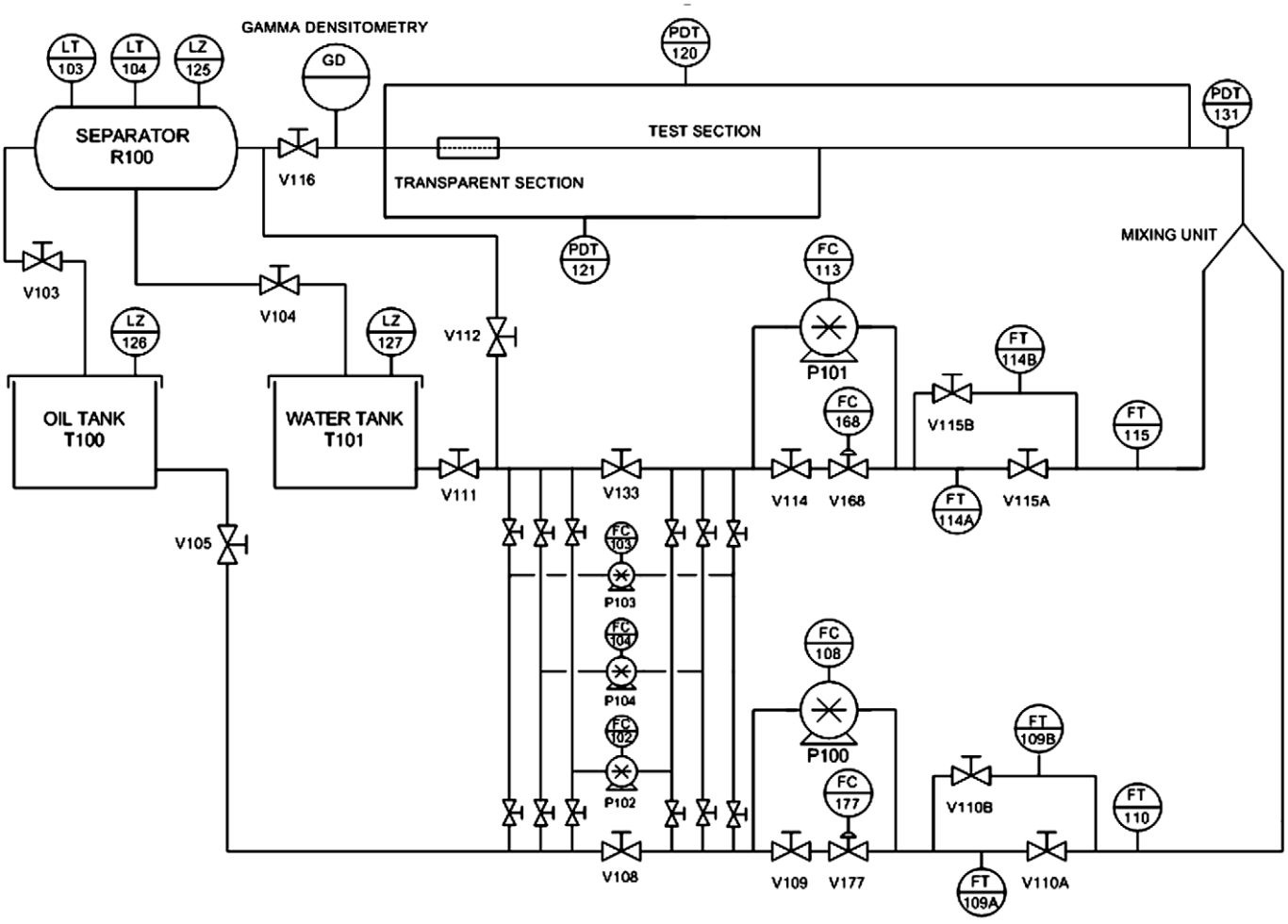

Fig. 2. Simplified flow sheet of the test rig.

Table 1
Physical properties of test fluids at 25 °C and 1 atm.

Liquid phase	Density (kg/m^3)	Viscosity (Pa s)	Surface tension (N/m)	Inter facial tension (N/m)
Water	996	0.001	0.07197	0.043
Exxsol D60 oil	790	0.00164	0.02530	

atmospheric outlet pressure. The physical properties of test fluids are listed in Table 1. The different techniques used for phase fraction and frictional pressure drop measurements are described below.

3.1. Single-beam gamma densitometry

The gamma densitometer is equipped with a radioactive source, detector and signal processing system as shown in Fig. 3a. The source and the detector are located diametrically opposite to each other on a pipe section. The source is mounted inside a lead shielding container. Both source and detection units are connected to a linear translation device in order to move them in the vertical direction, with a spatial resolution of 1 mm. This allows the averaged volume fractions to be measured over the whole pipe cross-section. A controller based on LabView® governs the traversing system and data acquisition.

There are many isotopes available, which emit gamma rays. The criteria for the selection of radiation source are; radiation energy (E_γ), half-life ($t_{1/2}$), cost and availability. The radiation energy of the source must satisfy two conflicting demands; accuracy of the measurements and safety. Strong sources avoid the problems posed by background radiation and may be used with large diameter pipes. The stronger sources also help to reduce the uncertainty in the counting statistics. However, for a high-energy source, thick shielding is required, and the large size of the instrument is thus a disadvantage to the applications where compactness is required. In addition, very strict safety precautions must be applied in handling strong radioactive sources. In general, radioactive materials with a long half-life are used as radiation sources to avoid frequent source replacements. In addition, frequent calibration measurements must be performed in order to account the rapid loss of intensity of radioactive source with a short half-life. Table 2 shows frequently used gamma radiation sources. Cs-137 sources are often used in conventional gamma-ray densitometers. Cs-137 source with radiation energy of 661.6 keV, requires about 10 cm of lead

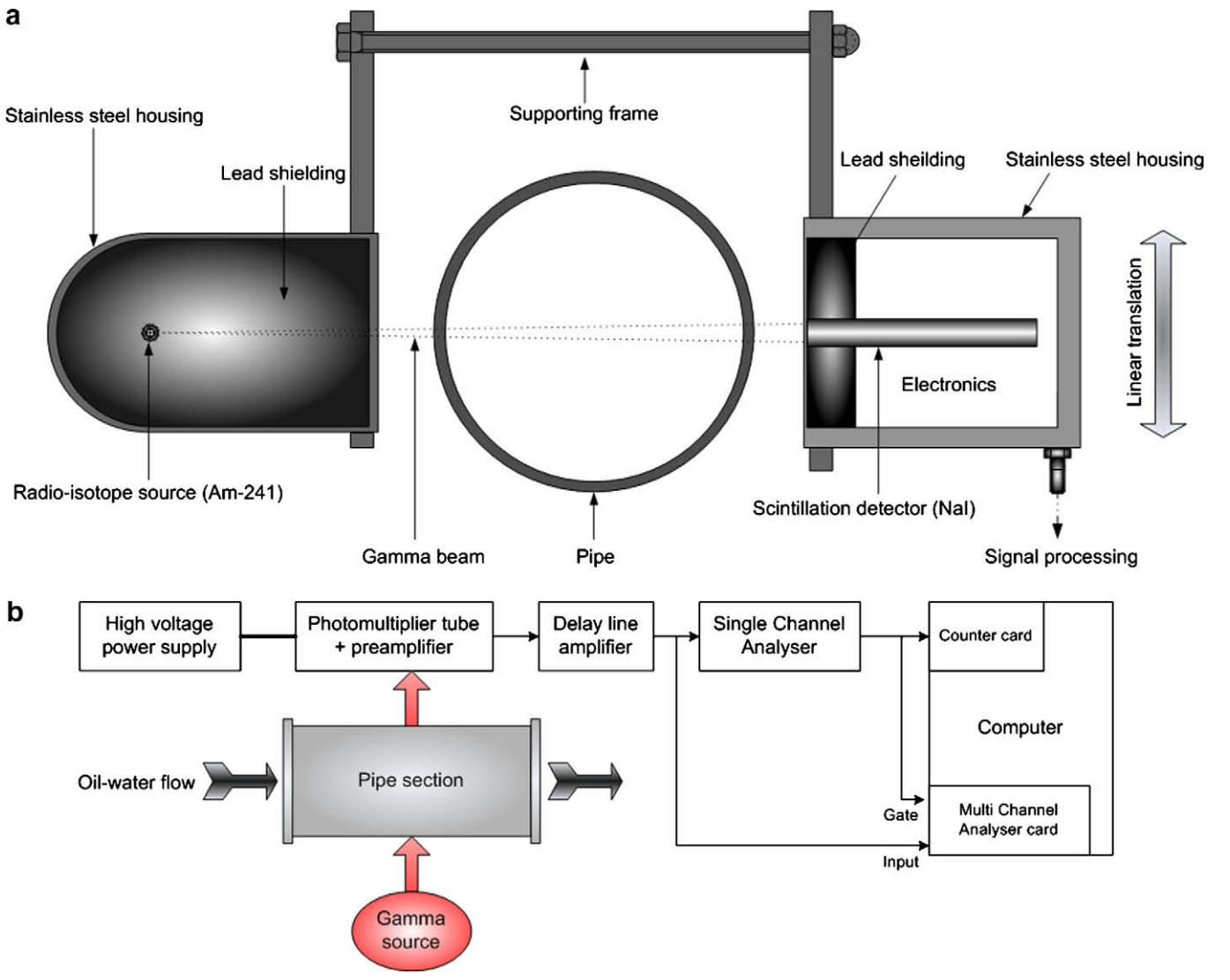

Fig. 3. Gamma densitometry: (a) schematic design of the gamma-ray densitometer, (b) schematic showing the principal components of the gamma-ray densitometer.

Table 2
Gamma-ray sources.

Isotope	Radiation energy (keV)	Half-life
Cs-137	661.6	30.2 years
Co-57	790	270 days
Ba-133	356	10.8 years
Am-241	59.5	433 years

shielding to meet the safety requirements. This makes the shield dimensions an obstacle for using this source in compact gamma densitometers. Co-57 source is not suitable since its short half-life makes frequent source replacements necessary. For the Ba-133 source 2–3 cm of lead shielding is needed. However, the difference between the mass absorption coefficients of oil and water becomes smaller at higher radiation energies (>100 keV), implying that oil and water phases are difficult to distinguish from each other (Pan, 1996). The lead shielding requirement is reduced to only 2 mm for the Am-241 source (Åbro and Johansen, 1998). In addition, it has a longer half-life of 433 years. The Am-241 source thus offers the best combination of radiation energy and activity over a longer period. In addition, Am-241 sources are readily available (Schlieper et al., 1987). Hence, Am-241 source (45 mCi) is used in the gamma densitometry for the present measurements. The gamma-ray emission is isotropic and fine collimator structure must be used to generate a narrow beam. In the present system, circular slot with diameter 3 mm and length 10 mm is used as the source collimator. The choice of Am-241 does not allow the use of pipe material with a significantly higher values of linear attenuation coefficients, as for example steel ($\kappa = 945\ m^{-1}$). Hence, a short polypropylene pipe section is used for gamma densitometry measurements. The linear attenuation coefficient of polypropylene is 17.90 m^{-1} at 59.5 keV (Tjugum et al., 2002).

For radiation detection, a thallium activated sodium iodide, NaI(Tl) scintillator is used. It has higher light output that yields good energy resolution and the detection efficiency is close to 100% for low energy gammas (<200 keV). However, it has relatively long decay times (230 ns). This sets a practical counting rate limit of about 10^5 counts per second. If this limit is exceeded, the scintillator will saturate and erroneous measurements would results. In order to stay within the counting rate limit, a less intense beam and longer counting times are required (Chan and Banerjee, 1981). In the present experiments, the observed maximum count rate is below 30,000 counts per second. Hence, the measured count rates are well below the maximum count rate (10^5 counts per second) where the detector becomes saturated. The detector is also collimated so that only transmitted radiation will be detected whereas scattered radiation can be neglected. The detector collimator is a rectangular slot with cross-section 3 × 10 mm and length 10 mm. The main components of signal processing system of the single-beam gamma densitometer are shown in Fig. 3b. Scintillation detector emits light when gamma rays interact with the atoms in the NaI(Tl) crystal. The intensity of the light produced is proportional to the energy deposited in the crystal by gamma radiation. The detector is connected to the photomultiplier tube (PMT). PMT is a photosensitive device consisting of a photoemissive cathode followed by focusing electrodes, an electron multiplier and an electron collector (anode) in a vacuum tube. When scintillation light impinges the photocathode, photoelectrons are emitted into vacuum by the photoelectric effect. The number of photoelectrons generated by one gamma ray interaction in the scintillator is far too low to be properly detected by the read-out electronics. Hence, the photoelectron signal is amplified directly in the second part of the PMT, the electron multiplier. It comprises focusing electrodes, a set of dynodes and an anode collecting electrons at the end. The focusing electrodes voltages direct the photoelectrons towards the first dynode, which is held at a potential of several hundred volts. Each photoelectron is thus accelerated to gain sufficient energy to cause emission of several electrons upon impact with the dynode. These electrons are then accelerated towards the next dynode where the number of electrons is further multiplied. This process is repeated at all dynodes and number of electrons collected at the anode is significantly larger than the number of initial photoelectrons. The highly intensified burst of electrons, arrives at the anode of the tube, still proportional to the energy of origin, is transferred to form a change at the input capacitor in the preamplifier. The preamplifier responds by creating a positive output pulse, which remains the basic proportional significance. The preamplifier is built together with photomultiplier tube. There are two inputs to the preamplifier. The anode output from the photomultiplier tube and the high voltage supply. The high voltage supply can furnish an output of ±1–1000 V DC. The output signal of the preamplifier has an amplitude depending on the input pulse and the high voltage supply. The signal from the preamplifier is fed into a delay line amplifier. It produces 100 ns long pulses from the exponential decaying pulses. Hence, the "chaos" from the preamplifier is turned into a sequence of pulses. After the delay line amplifier, a single channel analyzer (SCA) uses a discriminating window, consisting of a lower and upper voltage level, to filter this signal, in order to produce a logic output pulse for every incoming signal resulting from a photon of a particular energy. The SCA produces a logic output pulse if a pulse from the delay line amplifier is higher than the low level of the window and lower than the high level of the window. The gamma source emits photos at a range of energies. The background radiation produces low frequency scatter. In the entire range of frequencies detected by the photomultiplier tube, the dominant energy is the energy of the photon that is produced by the decaying process of Am-241 this is 59.5 keV. The dominant peak can be isolated with the electrical circuit producing measurements at a single energy level. However, nuclear sources may have a second or third less pronounced peaks. A multi channel analyzer (MCA) is used to find the number of photons received per second at every energy level. The multi channel analyzer is a PC containing an ORTEC TRUMP-PCI pulse height analyzer card run by the MAESTRO-32 MCA Emulation software package.

Photon count recording is initiated when the steady flow conditions are attained. As with all radiation measurement techniques, because of the statistical nature of the source, there is a compromise between measurement time and accuracy. The greater the accuracy required, the longer would be the measurement period. It is described in detail in the following. In the present work, photon count data collection is undertaken for a period of 50 s at each measurement site giving a measurement error of 0.97%.

3.2. Pressure drop measurements

The introduction of a small inclination in the pipeline causes the total pressure drop (dp_t/dL) to be a function of elevation as well as friction and acceleration as given below:

$$-\frac{dp_t}{dL} = -\frac{dp_f}{dL} - \frac{dp_a}{dL} - \frac{dp_g}{dL} \tag{9}$$

The terms on the right-hand side of the above equation are often designated as fictional (dp_f/dL), acceleration (dp_a/dL) and gravitational (dp_g/dL) components of the total pressure drop. The acceleration component has a negligible magnitude in oil–water flow systems (Flores et al., 1998) and the frictional component can be estimated by subtracting the gravitational component from the experimentally measured total pressure drop.

Rosemount® 3051 differential pressure transmitter (measurement range of 0–50 mbar) is used to measure the total pressure drop over the test section. The connection pipes to the pressure transmitter are filled with water. For inclined flows, the frictional

pressure drop can be estimated using the measured total pressure drop and corrections to account gravitational components due to the density difference in the pipe and water in the connection pipes. The frictional pressure drop in the present experimental set-up can be estimated as:

$$-\frac{dp_f}{dL} = -\frac{dp_t}{dL} - \rho_{mix} g \sin\xi + \rho_w g \sin\xi \tag{10}$$

where ρ_{mix} is the mixture density, g is the gravitational acceleration and L is the distance between the points where the pressure drop is measured. ξ is the pipe inclination angle from the horizontal. The last term in Eq. (10) is added to correct the pressure measurements due to the presence of water in the connection pipes. The mixture density could be calculated based on hold-up measurements from gamma densitometry (Elseth, 2001).

$$\rho_{mix} = \rho_w \eta_w + \rho_o (1 - \eta_w) \tag{11}$$

where η_w represents averaged water hold-up and it is described in detail in the following. The differential pressure transmitters are specially calibrated to handle negative values at low mixture velocities in upwardly inclined flows. The accuracy of the pressure measurements is ±0.1% of the measurement range, i.e. ±0.05 mbar.

3.3. Investigated flow conditions

The experiments were performed at three different mixture velocities 0.25, 0.50 and 1.00 m/s. The mixture velocity for oil–water flow is defined as:

$$U_m = \frac{Q_o + Q_w}{A} \tag{12}$$

where Q_o and Q_w are the inlet volumetric flow rates of oil and water, respectively and A is the pipe cross-sectional area. The water cut (λ_w) for oil–water flow is given as:

$$\lambda_w = \frac{Q_w}{Q_o + Q_w} \tag{13}$$

In the present work, the water cut is varied from 0 to 1. The experiments are performed at five different pipe inclinations (−5°, −1°, 0°, +1° and +5°).

4. Results

The effects of pipe inclination on the water hold-up, slip ratio and frictional pressure drop of oil–water flow are investigated in this section.

4.1. Calibration of gamma densitometer

The gamma densitometer must be calibrated as precursor to two-phase oil–water flow measurements. For this purpose, the reference gamma counts for the individual test fluids are determined in static conditions. The test pipe is filled with each test fluid and gamma count rates are recorded. Fig. 4a shows single-phase calibration curves for oil and water phases. The number of counts (or intensity) received is plotted on the x-axis and the normalized radial position of the pipe is plotted on the y-axis. The measured radiation intensity for oil is higher than water due to lower linear attenuation coefficient. The gamma densitometry results are validated with static two-phase data prior to the flow measurements. In this case, the measurements are performed on a stratified oil–water mixture with water cut 0.50, and the results are presented in Fig. 4. As shown in Fig. 4a, the two-phase case follows the intensity measurements for pure water up to the normalized radial position −0.08 and it follows intensity measurements for the oil from the normalized radial position 0.05. The intensity varies from pure

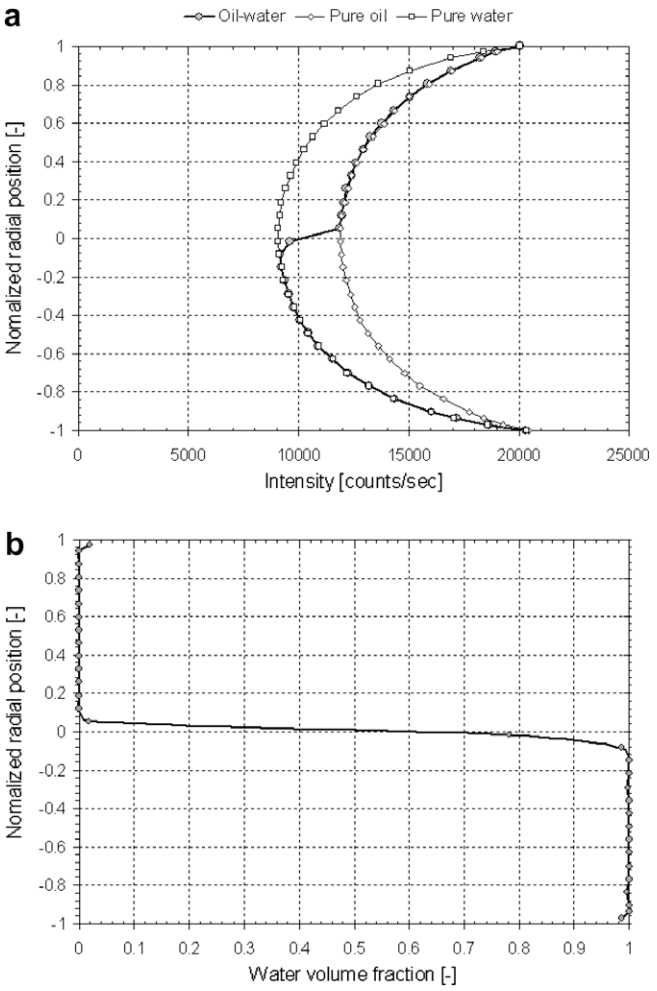

Fig. 4. Gamma densitometry measurements: (a) raw data, (b) water volume fraction measurements.

water to pure oil across the interface. The raw intensity data can be converted into chordal averaged water volume fractions using Eq. (7) and the results are presented in Fig. 4b. The water volume fraction is expected to be zero in the oil phase and one in the water phase. At the interface it will be somewhere in between. The measured water volume fraction is about 0.50 at the center of the pipe. Good agreement between measurements and visual observations can be seen except for the measurement points close to the wall. While measuring close to the pipe wall, parts of the gamma beams hit the wall instead of the flow, making the control volume very small. The accuracy of the gamma densitometer decreases with decreasing control volume, and severely reduced accuracy is expected in the measurements closest to the pipe wall. This will be discussed in detail under the section of uncertainty analysis in the latter part of the paper.

4.2. Water hold-up and slip ratio measurements

The water hold-up (η_w) for oil–water flow can be defined as the fraction of water in a given section of pipe. It can be estimated as:

$$\eta_w = \frac{A_w}{A} \tag{14}$$

where A_w is the cross-sectional area occupied by the water phase. In stratified flow, the vertical distance from the bottom of the pipe to the point where the local water volume fraction is equal to 0.50 is

considered as the interface height and the interface is treated as a flat surface in order to estimate the flow areas for different phases. It is possible to measure the liquid fractions as function of time at a given cross-section of the pipe: the so-called in situ water hold-up. In oil–water flows, the in situ hold-up will be time-dependent due to, for example, wavy motion and mixing at the interface. An averaged hold-up value can be obtained by taking some average of the time-dependent signal. The water hold-up values reported in this paper are estimated using time averaged water volume fraction measurements from gamma densitometry.

The slip between the phases is a typical phenomenon, which occur in liquid–liquid flows in pipes as well as in other multiphase systems. The ratio between the averaged in situ velocities of the two phases is often given as slip ratio, S, and it can be calculated as:

$$S = \frac{U_o}{U_w} = \frac{A_w}{A_o}\frac{U_{so}}{U_{sw}} \tag{15}$$

where A_o is the flow area occupied by the oil phase. U_{so} and U_{sw} are superficial velocities for oil and water phases, respectively. The superficial velocities for different phases are defined as follows:

$$U_{so} = \frac{Q_o}{A} \quad \text{and} \quad U_{sw} = \frac{Q_w}{A} \tag{16}$$

The slip ratio depends on physical properties combined with flow rates, flow pattern and pipe geometry. $S > 1$ means that the oil phase travels faster than the water phase in the pipe while $S < 1$ indicates that water is the faster phase.

The measured water hold-up and slip ratio data for different pipe inclinations and inlet water cuts are presented at mixture velocity $U_m = 0.25$ m/s in Fig. 5. It is important to note that the hold-up, which is measured, is in almost all instances significantly different from the input water cut as shown in Fig. 5a. In upward flow, there is an expected trend of in situ accumulation of the denser phase, in this case water. When the pipe is inclined downwards, lower water hold-up values are observed compared to the horizontal flow. In addition, the water hold-up is very dependent on the pipe inclination when the pipe is nearly horizontal (+1° and −1°). The water hold-up increase from 0° to +1° appears greater than from +1° to +5°. At the higher pipe inclination (+5°), high water hold-up is still favoured but is tempered slightly by the wavy flow pattern and increased mixing at the interface. Fig. 6 shows the flow patterns observed for different pipe inclinations at mixture velocity 0.25 m/s and water cut 0.50. Fig. 6a illustrates the smoothly stratified flow in the horizontal pipe. At pipe inclination is +1°, some mixing at the interface is recorded. Nevertheless, oil and water phases are clearly stratified and large interfacial waves are not observed as shown in Fig. 6b. Higher mean axial velocities are observed in the oil phase compared to the water phase at pipe inclination +5° (Kumara et al., 2009b). As a result, the pressure in the oil phase over the interface decreases owing to the Bernoulli effect, and this tends to cause the interfacial waves to grow (Brennen, 2005). Bernoulli forces depend on the differences in the velocity of the two streams, $\Delta u = u_o - u_w$ and are characterized by $\rho(\Delta u)^2 l^2$, where ρ and l are a characteristic density and dimension of the flow. Hence, for low mixture velocities at pipe inclination +5° stratified wavy flows are observed as shown in Fig. 6c. The wavy interface tempered the increase in the water hold-up from pipe inclination +1° to +5°. At pipe inclination −1°, stratified flow is observed without interfacial waves and mixing at the interface as shown in Fig. 6d. The water hold-up significantly decreases compared to the horizontal flow due to increased water velocity. At pipe inclination −5° water phase has significantly higher mean axial velocities compared to the oil phase (Kumara et al., 2009b). As a result, water phase tends to disperse the oil phase and thick interface region is observed as shown in Fig. 6e. Hence, the decrease in the water hold-up from −1° to −5° is moderated compared to from 0° to −1°.

Fig. 5b presents slip ratio measurements for different pipe inclinations and inlet water cut at mixture velocity $U_m = 0.25$ m/s. At this low mixture velocity, stratified flows are observed, except for higher water cuts (>0.925) at pipe inclination +5°. For stratified flow, the slip ratio varies widely with the water cut. Hence, the logarithmic scale is used on the y-axis. At pipe inclination +5°, the slip ratio shows a clear decreasing trend with increasing water cut. The calculated slip ratio is 24.5 at inlet water cut 0.025 and it reduces to 1.5 at inlet water cut 0.90. For horizontal flows, it varies from 2.3 to 0.3 as the inlet water cut varies from 0.025 to 0.975. The slip ratio of downwardly inclined pipes varies over a wider range compared to the horizontal pipes. At pipe inclination −5°, the estimated slip ratios are 1.3 at water cut 0.025 and 0.03 at water cut 0.975. For low water cuts, the oil moves faster than the water due to the difference in wetted perimeters giving $S > 1$. For higher water fractions, the slip ratio becomes lower and the water velocity becomes higher than the oil velocity, i.e. $S < 1$. The measured slip ratio is equal to one at water cut 0.60 for horizontal flow and equal to one at water cut 0.90 for pipe inclination +1°. Oil, as the

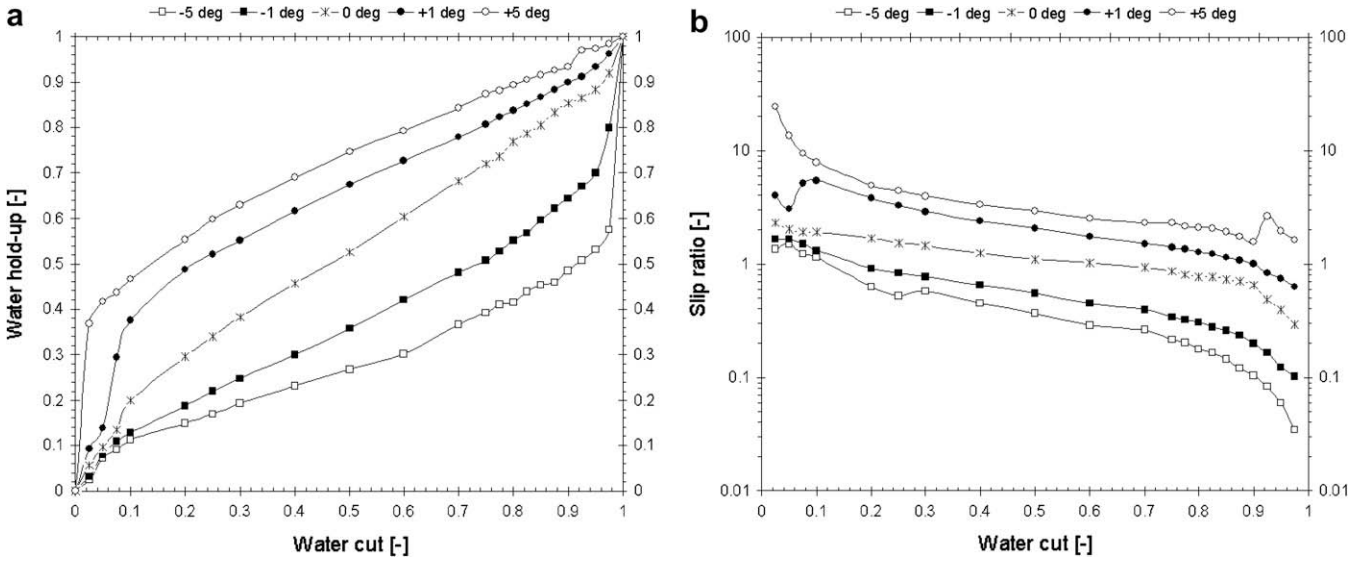

Fig. 5. Mixture velocity, $U_m = 0.25$ m/s: (a) water hold-up, (b) slip ratio.

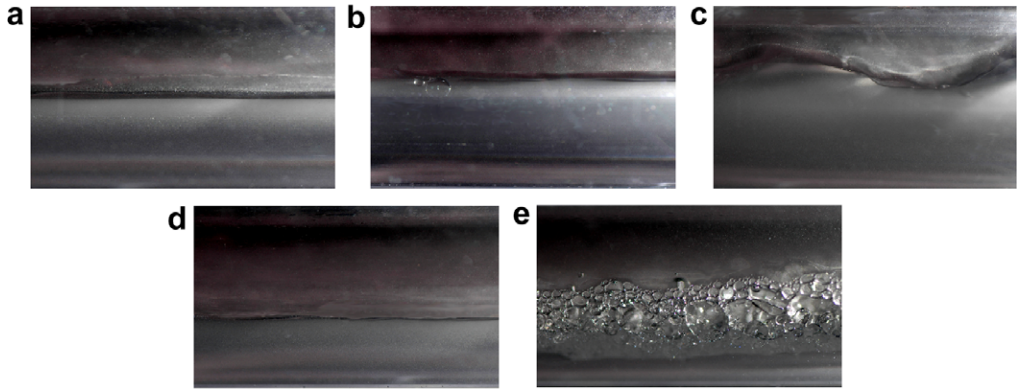

Fig. 6. Different flow patterns at mixture velocity 0.25 m/s and water cut 0.50 for different pipe inclinations: (a) 0°, (b) +1°, (c) +5°, (d) −1°, (b) −5°.

less dense phase, travels at a considerably higher velocity than water, so that the slip ratio is always above one for upwardly inclined pipe at +5°. In downwardly inclined oil–water flows, the gravity would favour faster water flow and the slip ratio is below one over a wide range of water cuts. The slip ratio is above one up to the water cuts approximately 0.18 and 0.13 for pipe inclinations −1° and −5°, respectively. An increase in slip ratio values is observed at pipe inclination +5° at higher inlet water cuts ($\geqslant$0.925). At these flow conditions, a time-dependent plug flow regime is observed that gives some fluctuations in time averaged gamma densitometry measurements. The separation of oil plugs from the continuous oil layer starts at water cut 0.925. This flow pattern has been observed previously by Lum et al. (2006) in upwardly inclined oil–water flows. Some fluctuations in measured slip ratio is observed at pipe inclination +1° at lower inlet water cuts (<0.075), due to increased mixing.

The measured water hold-up values at mixture velocity 0.50 m/s for upwardly and downwardly inclined pipes at different water cuts are given in Fig. 7a. The water hold-up values show a narrow variation compared to the results at lower mixture velocity, U_m = 0.25 m/s as shown in Fig. 5a. For upwardly inclined flows, the accumulation of water phase due to the gravity is decreased at higher mixture velocities due to the increased momentum transfer between the phases giving lower water hold-up values. At higher water cuts, oil is dispersed in water and oil-in-water dispersion is formed and flows over the water layer for all the pipe inclinations. The degree of mixing is higher for upwardly and downwardly inclined pipes compared to the horizontal flow. This mixing effect at higher water cuts gives lower variations in measured water hold-up values for different pipe inclinations.

The estimated slip ratio data at mixture velocity, U_m = 0.50 m/s, is given in Fig. 7b. The slip ratio is also varying in a narrow range in compared to the results at low mixture velocities. At pipe inclination +5°, oil phase is moving faster than the water phase up to the water cut 0.85, i.e. $S > 1$. At higher water cuts, oil phase is dispersed in water and accumulated at the upper part of the pipe. Although the discrete oil droplets could move somewhat faster than the surrounding water, their average velocity may still be less than the averaged water velocity, which also takes into account the faster moving water at the center of the pipe. Hence, the slip ratio is less than one at higher water cuts at pipe inclination +5°. As the pipe inclination decreases the slip ratio decreases. At pipe inclination −5°, the water phase moves faster than the oil phase, as the water cut increases above 0.050.

The measured water hold-up as a function of inlet water cut at mixture velocity 1.00 m/s for different pipe inclinations is given in Fig. 8a. In this case the water hold-up values for horizontal and nearly horizontal (−1° and +1°) flows show marginal differences. This is due to increased momentum transfer between the oil and water phases at higher mixture velocities. Nevertheless, the water

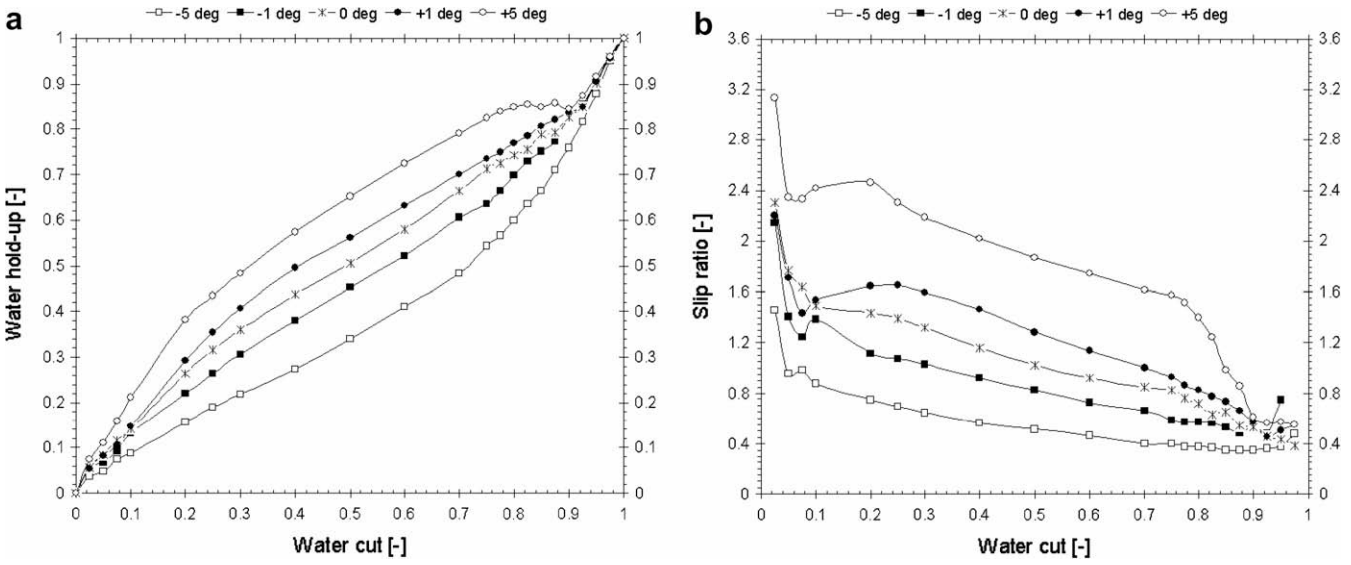

Fig. 7. Mixture velocity, U_m = 0.50 m/s: (a) water hold-up, (b) slip ratio.

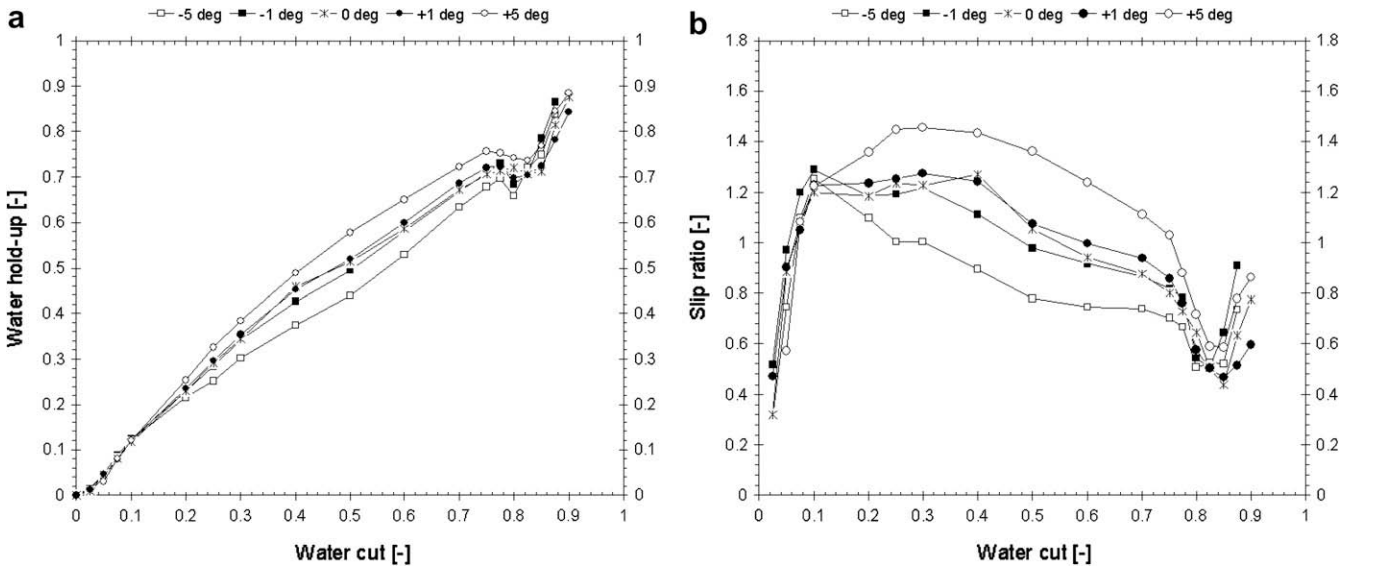

Fig. 8. Mixture velocity, U_m = 1.00 m/s: (a) water hold-up, (b) slip ratio.

hold-up values at pipe inclination +5°, is slightly higher compared to the horizontal flow at intermediate inlet water cuts ($0.10 < \lambda_w < 0.80$). On the other hand, it is slightly lower for downwardly inclined flow at −5° compared to the horizontal flow. At low water cuts (<0.075) water phase is dispersed in oil and hold-up profiles for different pipe inclinations are closely fallen together. On the other hand, at high inlet water cuts (>0.80) oil phase is dispersed in water and some fluctuations in measured hold-up values are observed.

The slip ratio measurements at U_m = 1.00 m/s is given in Fig. 8b. At higher mixture velocities, the slip ratio varies over a narrow range around $S = 1$, due to increased level of mixing between oil and water phases. At low water cuts, increased mixing reduces the slip between phases. As the inlet water cut increases, the sedimentation and coalescence of water droplets increases making a continuous water layer at the bottom of the pipe. Therefore, the dual continuous flows are observed at intermediate inlet water cuts ($0.10 < \lambda_w < 0.80$). The measured slip ratio at pipe inclination +5° is higher than the measured values for pipe inclinations +1° and 0°, due to increased water hold-up. In addition, the slip ratio measurements at pipe inclination −5° are lower than the measurements at −1° and 0°. At higher water cuts, smaller slip ratio values are observed.

The water hold-up and slip ratio measurements of oil–water flow in horizontal and inclined pipes have been reported by many researchers as shown in Table 3. However, the previous investigations differ from the current work in inclinations, pipe diameters, fluid properties and flow velocities used. Hence, only a general comparison can be performed. Scott (1985), Lum et al. (2002), Abduvayt et al. (2004) and Lum et al. (2006) studied oil–water flows in upwardly inclined pipes. These investigators have reported higher water hold-up values in upwardly inclined pipes than horizontal pipes. In general, the slip ratio increases with pipe inclination (Lum et al., 2006). All the slip ratio measurements presented by Scott (1985) and most of those by Lum et al. (2002) and Abduvayt et al. (2004) are in general above one. Lum et al. (2006) have reported slip ratio values below one at mixture velocity 1.00 m/s at higher water cuts. Previous studies also show that slip ratio approaches one with increasing mixture velocity, due to the higher level of mixing (Scott, 1985; Lum et al., 2002, 2006; Abduvayt et al., 2004). The present slip ratio measurements show a good consensus with previous investigations.

For downwardly inclined oil–water flows, Abduvayt et al. (2004) showed that slip ratios are always less or equal to one, while Cox (1985) found generally low slip ratios, although not always below one. Lum et al. (2006) presented slip ratios both above and below one. They observed that slip ratio is generally closest to one at −5°, due to higher level of dispersion and the effect of gravity. Slip ratios slightly below one have been observed at lower water cuts at mixture velocity 2.00 m/s. In the present study, slip ratios above one are observed at low water cuts at mixture velocity 0.25 m/s and 0.50 m/s. In general, smaller slip ratios are observed for downwardly inclined pipes. Hence, the present measurements show a good agreement with data presented by Cox (1985) and Lum et al. (2006) for downwardly inclined oil–water flows.

4.3. Pressure gradient measurements

Fig. 9 presents the frictional pressure drop as a function of water cut for five different pipe inclinations at mixture velocity 0.25 m/s. It is important to note that, despite the oil being more viscous phase, single-phase water flow presents a slightly higher frictional pressure drop in comparison with single-phase oil flow. In this case, the Reynolds numbers for single-phase oil and water flows are 6744 and 13,944, respectively. Hence, the water has higher turbulent intensity, which results in a higher effective viscosity, thereby higher frictional pressure drop. At this low mixture velocity, stratified flows are observed except at higher and lower inlet water cuts in inclined pipes. There is little variation of pressure drop with water cuts. However, at higher water cuts some fluctuations are observed due to mixing at the interface. There are marginal differences in frictional pressure drop measurements for pipe inclination −5°, −1°, 0° and +1°. Higher frictional pressure drop values are observed at pipe inclination +5° compared to the other pipe inclinations. This can be directly attributed to the increased turbulence level due to stratified wavy flow pattern observed at pipe inclination +5° (see Fig. 6c). Kumara et al. (2009b) investigated the turbulence structure in wavy oil–water flow at mixture velocity 0.25 m/s for different pipe inclinations. The results showed that the interfacial waves cause an increase in the turbulent intensities and Reynolds stress. Hence, the turbulent level is significantly increased in stratified wavy flows in comparison with smoothly stratified flows. This higher turbulence production in stratified wavy flows extracts more energy from the mean flow.

Table 3
Oil–water flow experiments in pipes.

Authors	ID (mm)	Inc (°)	Superficial velocities (m/s)		Physical properties					Measured flow properties
			Oil	Water	Oil		Water		σ_{ow}	
					ρ (kg/m^3)	μ (mPa s)	ρ (kg/m^3)	μ (mPa s)	(mN/m)	
Cox (1985)	50.8	−15 −30	0.05–0.64	0.05–0.64	754	1.38	998	0.894	N/A	Water hold-up Slip ratio Pressure drop
Scott (1985)	50.8	+15 +30	0.05–0.64	0.05–0.64	754	1.38	998	0.894	N/A	Water hold-up Slip ratio Pressure drop
Nädler and Mewes (1997)	59	0	0.014–1.44	0.009–1.48	841	31	998	1	N/A	Pressure drop
Valle and Utvik (1997)	77.9	0	0–2.33	0–2.33	791	1	1000	0.43	28.5	Water hold-up Slip ratio Pressure drop
Angeli and Hewitt (1998)	24.3	0	0.3–3.9	0.3–3.9	801	1.6	1000	1	17	Pressure drop
Alkaya (2000)	50.8	±5 ±2 ±1 ±0.5	0.025–1.75	0.025–1.75	847.7	12.9	994.12	0.72	16.7	Water hold-up Pressure drop
Elseth (2001)	56.3	0	0.3–1.51	0.1–1.2	790	1.6	1000	1.02	43	Water hold-up Slip ratio Pressure drop Velocity and turbulence
Lum et al. (2002)	38	0 +5	0.07–2.25	0.07–2.25	828	5.25	998	0.993	40	Water hold-up Slip ratio Pressure drop
Abduvayt et al. (2004)	106.4	±3 ±0.5 0 90	0.025–1.502	0.025–1.502	800	1.88	1000	1.0	N/A	Water hold-up Slip ratio Pressure drop
Lum et al. (2006)	38	−5 0 +10	0.07–2.78	0.07–2.78	828	5.5	998	0.993	40	Water hold-up Slip ratio Pressure drop

N/A – not available.

Thus, higher frictional pressure drops are observed. At pipe inclination, +1° and −1° stratified flows are mainly observed with some mixing at the interface. Large interfacial waves are not observed. Hence, marginal differences in frictional pressure drop are observed. The measured frictional pressure drop at pipe inclination −5° is very similar to the measured pressure drop for horizontal flow up to the inlet water cut 0.70. In this case, stratified flow with some mixing at the interface is observed without large interfacial waves. Nevertheless, slightly higher frictional pressure drop values are observed at higher water cuts. The oil–water interface is highly disturbed due to increased level of mixing at higher water cuts at pipe inclination −5° compared to the horizontal flow. This would have led to higher frictional pressure gradients.

Frictional pressure drop measurements for different inclinations at mixture velocity, U_m = 0.50 m/s, are presented in Fig. 10. One rather striking behavior of the frictional pressure drop in oil–water flow is observed at higher water cuts, as the mixture velocity increases from 0.25 m/s to 0.50 m/s. The frictional pressure drop increases quite dramatically at higher water cuts. At high water cuts, all the oil is dispersed and appears in the form of droplets in the water continuous matrix. The increase in the measured pressure gradient is a result of an increased effective (or emulsion) viscosity resulting from interaction of the dispersed droplets. The peak in pressure drop is observed at inlet water cut equal to 0.90 for horizontal flow. The frictional pressure drop profiles for other pipe inclinations also show same overall trend as horizontal flow.

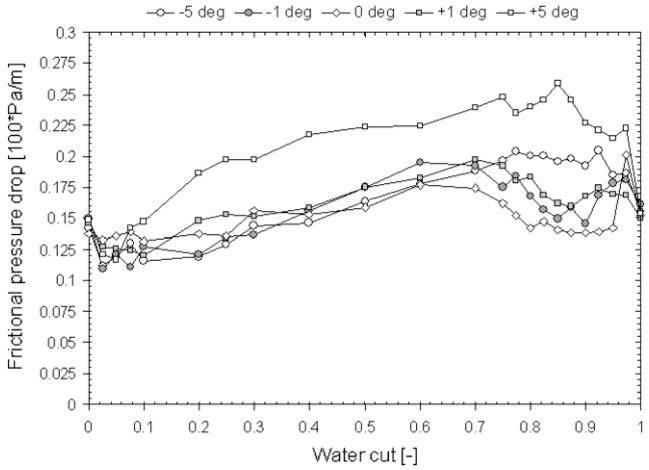

Fig. 9. Frictional pressure drop as a function of water cut: U_m = 0.25 m/s.

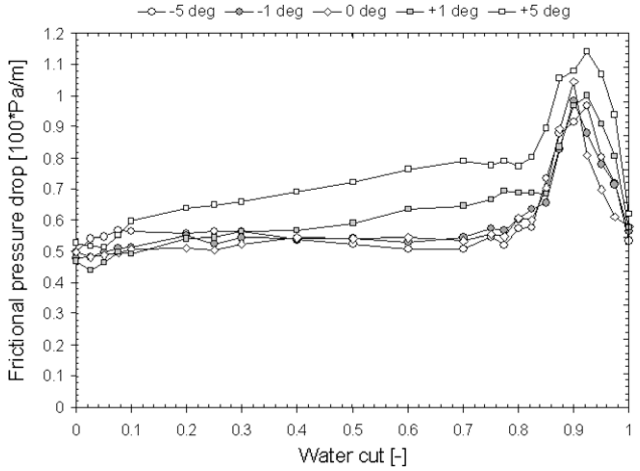

Fig. 10. Frictional pressure drop as a function of water cut: U_m = 0.50 m/s.

The peaks in pressure drop for other pipe inclinations are located between the water cuts 0.90 and 0.925. Nädler and Mewes (1997) investigated that phase inversion takes place within the dispersion layer and hence only in a restricted area of the pipe. The higher frictional pressure gradients that they have observed at higher water cuts have been attributed to the partial inversion effect. Elseth (2001) has also reported a similar behavior of the frictional pressure drop of oil–water flow in horizontal pipes in comparison with present results. Again slightly higher frictional pressure drop values are observed for upwardly inclined pipes due to the higher turbulence level associated with interfacial waves. There are marginal differences in frictional pressure drop measurements between horizontal and downwardly inclined flows.

Fig. 11 represents the frictional pressure drops at mixture velocity at 1.00 m/s for different pipe inclinations. The peak is observed at about inlet water cut 0.81 for all the pipe inclinations. At higher mixture velocities, oil is dispersed in water at lower water cuts compared to low mixture velocities. Therefore, the peak in pressure drop is observed at lower water cut at higher mixture velocities. The frictional pressure drop measurements at pipe inclinations −5°, −1°, 0° and +1° are generally very similar, in terms of both the trends and the absolute values. However, slightly higher frictional pressure drops are observed at pipe inclination +5° due to interfacial waves.

Frictional pressure drop measurements of oil–water flow in horizontal flows have been presented by many investigators as shown in Table 3. A peak in pressure drop around the point of phase inversion (approximately at inlet water cut 0.40) as observed by Angeli and Hewitt (1998) is not seen in any of the experiments. Most likely, the mixture velocity is too small for the expected peak to appear and the mixing unit at the entrance of the test section is designed in a way that reduces dispersions (Kumara et al., 2009a). The present pressure measurements for horizontal oil–water flow closely follow the data presented by Elseth (2001) and Nädler and Mewes (1997). The behavior of the frictional pressured drop of oil–water flow in inclined pipes is not well documented and the available data do not show a good agreement with each other. Alkaya (2000) has observed marginal differences between the frictional pressure drop measurements for horizontal and inclined flows. Lum et al. (2004) presented frictional pressure gradient data at 0° and +5° for mixture velocities 1.00 m/s and 2.00 m/s. They have observed little variations of pressure drop with water cut at mixture velocity 1.00 m/s for both horizontal and upwardly inclined flows. In addition, the measured frictional pressure drops for upwardly inclined pipes are slightly lower compared to the horizontal flow. Lum et al. (2006) have reported frictional pressure drop measurements of oil–water flow at different pipe inclinations (−5°, 0°, +5° and +10°) for different mixture velocities from 0.70 m/s to 2.50 m/s. They have found the frictional pressure drop to be lower in two-phase flow than in single-phase oil flow for all the inclinations investigated. The frictional pressure gradients in both upward and downward flows were lower than in horizontal flow despite the similarity in the flow patterns. They have observed little variations in frictional pressure drop with inlet water cuts at lower mixture velocities. The results of Abduvayt et al. (2004) showed an increase in the total pressure drop with pipe inclination. The present measurements show an increase in frictional pressure drop for upwardly inclined flow due to increased turbulence level associated with interfacial waves. However, marginal differences in frictional pressure drop are observed between horizontal and downwardly inclined flows.

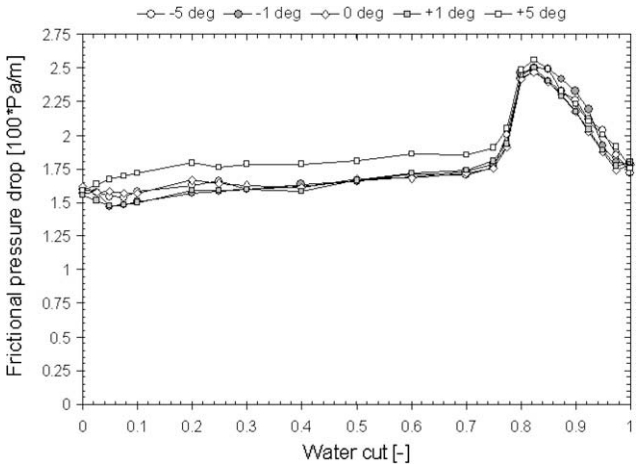

Fig. 11. Frictional pressure drop as a function of water cut: U_m = 1.00 m/s.

4.4. Uncertainty analysis

There are several sources of uncertainty that must be accounted for and minimized when making gamma densitometry measurements. In general, they can be listed as follows:

- Nonlinear detector response due to dead time.
- Background noise.
- Statistical uncertainty in photon counts.
- Uncertainties due to dynamic fluctuations of the flow field.
- Uncertainties due to geometric volume fraction distribution assumptions.

The problems related to the dead time of scintillation detectors are discussed in detail by several authors (Müller, 1973; Reda et al., 1981). The detector converts each individual gamma photon into a light pulse, which is detected using a photomultiplier tube. The light energy emitted rises sharply as a function of time until it reaches a maximum and then begins to decay exponentially. The system thus has an inherent time scale τ and measurements at rates comparable to or exceeding $1/\tau$ will not directly yield accurate count rates. Reda et al. (1981) provided measurements indicating τ = 3–5 μs, where the observed nonlinear response is fitted to the following model:

$$I_{act} = \frac{I_{obs}}{1 - \tau I_{obs}} \tag{17}$$

I_{obs} is the observed or measured intensity and I_{act} is the actual intensity in counts per second. In the present experiments, τ has been estimated by first obtaining single-phase gamma scans at known locations. The ratio of the single-phase count rates at each location is then compared to the expected attenuation predicted using the exponential decay law, with known path lengths. Finally, the nonlinear model given above by Reda et al. (1981) is used to correct for the deviation between the expected and observed values. τ was estimated to be 0.04 μs for the present system. Fig. 12 shows the effect of τ on the present measurements. It shows how well the curve fit used to determine τ agrees with the data and illustrates that τ may be smaller for present system than for previously reported values because the data does not extended very far into the nonlinear regime which would be required to make a better estimate of τ. The measured count rates are well within the linear response region of the detector. Thus, for the current set of operating conditions, measured intensities or count rates do not need to be corrected using τ to yield accurate values.

The presence of background noise due to electrical noise and background radiation should be accounted. It is estimated by recording count rates when the source is closed. It represents a systematic bias in the signal that will increase all count rates by approx-

imately the same amount in the linear response region of the detector. In the present system, the observed maximum count rate due to background noise is 1.5 counts per second, which represents in an uncertainty of less than 0.006%. Since this count rate is negligible and it was not subtracted from the experimental measurements.

The total measurement error (σ_{tot}) depends on the following sources of errors; statistical error (σ_{stat}), dynamic fluctuations of the flow field (σ_{flow}) and geometric volume fraction distribution assumptions (σ_{geo}). Moffat (1988) has given the correlation of these independent sources of uncertainty as:

$$(\sigma_{tot})^2 = (\sigma_{stat})^2 + (\sigma_{flow})^2 + (\sigma_{geo})^2 \tag{18}$$

The statistical error is the fundamental uncertainty that exists due to the random nature of photon emission by radioactive sources. This error is called the random photoemission error (Elseth, 2001). The error due to dynamic fluctuations of the flow field (σ_{flow}) is caused due to the changes of the volume fraction profile during the measurements. Although the measurements are taken in the region of quasi-steady flows, dynamic fluctuations often exist in oil–water flows. They are negligible for stratified, wavy and bubble flows, but the contribution of σ_{flow} to the total measurement error can be expected in the order of statistical error for slug and plug flow (Stahl and Rohr, 2004). In the present measurements, plug flow regime is observed only for higher water cuts ($\lambda_w > 0.925$) at mixture velocity 0.25 m/s in upwardly inclined pipe at +5°. The rest of the gamma measurements are performed with segregated or dispersed flows where σ_{flow} has a negligible influence on the total measurement error. In the case of geometrically complex flow patterns, it is necessary to use approximations to calculate the volume fractions from the measured radiation attenuation data. Typically used approximations are exponential or linear attenuation models, as discussed earlier. The measurement errors associated with these approximations (σ_{geo}) for different flow regimes were reported in detail by Stahl and Rohr (2004). They have found that the linear approximation is more appropriate for flow patterns whose phase interfaces are mainly oriented parallel to the radiation, while profiles with perpendicular interfaces or disperse flow patterns can be better approximated logarithmically. However, they have also reported that the logarithmic approximation can produce better results within the range of the statistical error for all the flow patterns except slug flow. In the present work, the same approach is adopted. Therefore, it can be concluded that the σ_{flow} and σ_{geo} have a contribution to the total measurement error, which is less significant than the statistical error for stratified, wavy and dispersed flow, where the present measurements are mainly performed.

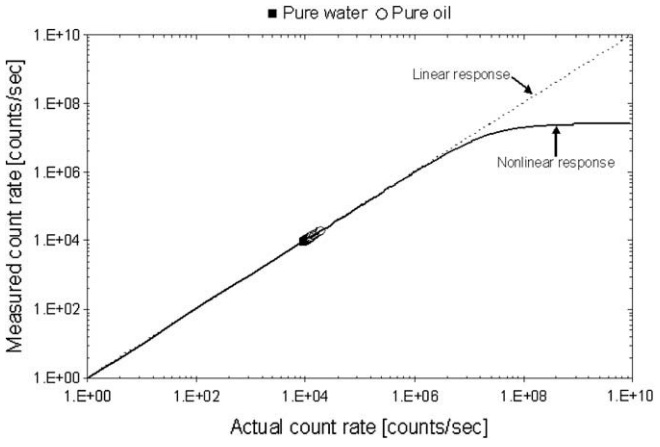

Fig. 12. Linear and nonlinear response of scintillation detector.

Pan (1996) has given a correlation in order to estimate the random photoemission error associated with gamma densitometry as given below:

$$\sigma_{stat} = \frac{\pm 1}{H(\mu_w\rho_w - \mu_o\rho_o)\{tI_0 \exp[-\mu_{wall}\rho_{wall}H_{wall} - (\mu_w\rho_w\varepsilon_w + \mu_o\rho_o(1-\varepsilon_w))H]\}^{0.5}} \tag{19}$$

where H and H_{wall} represent total (wall + oil + water) and wall distance traveled by the gamma beam, respectively. t and I_0 represent the measuring time and incident intensity (counts per second) of the gamma beam. As can be seen in Eq. (19) a total number of eleven parameters influence the statistical error of the measurements. Nevertheless, μ_w, μ_o and μ_{wall} are not independent variables because it is known that the mass absorption coefficient for a given substance depends on the gamma energy, E_γ. The measurement error is finally determined by nine independent parameters: t, E_γ, H, I_0, x_{wall}, ε_w, ρ_w, ρ_o and ρ_{wall} (Pan, 1996). The fluid densities and the density of the pipe material are already specified for a given system and the phase fraction, ε_w, simply varies with the flow conditions. It is straightforward to identify the optimum values for some of the parameters. For, instance the measuring time should be as large as practicable. In this section the effect of measuring time, radiation energy and beam position on the measurement error will be investigated further.

The gamma radiation emitted during the nuclear decay of radioactive source of Am-241 having a long half-life has an approximately constant count rate. The nuclear decay itself, however, is a statistical process giving a fundamental inaccuracy in the measurements due to the normal photon fluctuations (Schlieper et al., 1987). According to the Eq. (19), the measurement error is inversely proportional to the measuring time:

$$\sigma_{stat} = \frac{K}{\sqrt{tI_0}} = \frac{K}{\sqrt{N}} \tag{20}$$

where K is a constant for a given system and N is the total photon count acquired at a given measurement site. The measurement error decreases as the number of counts increases. Hence, a sufficient number of counts are required to achieve a higher accuracy of measurements. The effect of measuring time on the accuracy can be estimated assuming constant linear attenuation coefficients for fluids and wall material, fixed gamma beam across the pipe center and $\varepsilon_w = 1$, where ε_w is phase fraction of most absorbing phase, in this case water. In Fig. 13a, the measurement error is given as a function of the measuring time. The accuracy improves continuously with increasing measuring time. The measurement error is significantly higher for short measurement periods. In the present experiments, gamma counts are recorded for 50 s at each measurement point, giving a measurement error of 0.97%.

The mass absorption coefficients of oil and water in Eq. (19) are uniquely determined by the gamma radiation energy as discussed earlier, i.e. $\mu = \mu(E_\gamma)$. Hence, the measuring error of phase fraction measurements in a given two-phase system is strongly dependent on radiation energy level. For the oil–water system, the measurement error as a function of radiation energy is given in Fig. 13b. The estimation is carried out assuming fixed incident radiation intensity (28,400 counts/s) and constant linear attenuation coefficient of wall material. The gamma beam is positioned across the pipe center and the measuring time is 50 s. It is further assumed that, $\varepsilon_w = 1$. As can be seen in the figure, the error increases as the radiation energy increases. The marginal difference between mass absorption coefficients of oil and water at higher radiation energy levels gives significant measurement errors. The present set-up with Am-241 source having radiation energy, $E_\gamma = 59.5$ keV, gives measurements with an error of 0.54%.

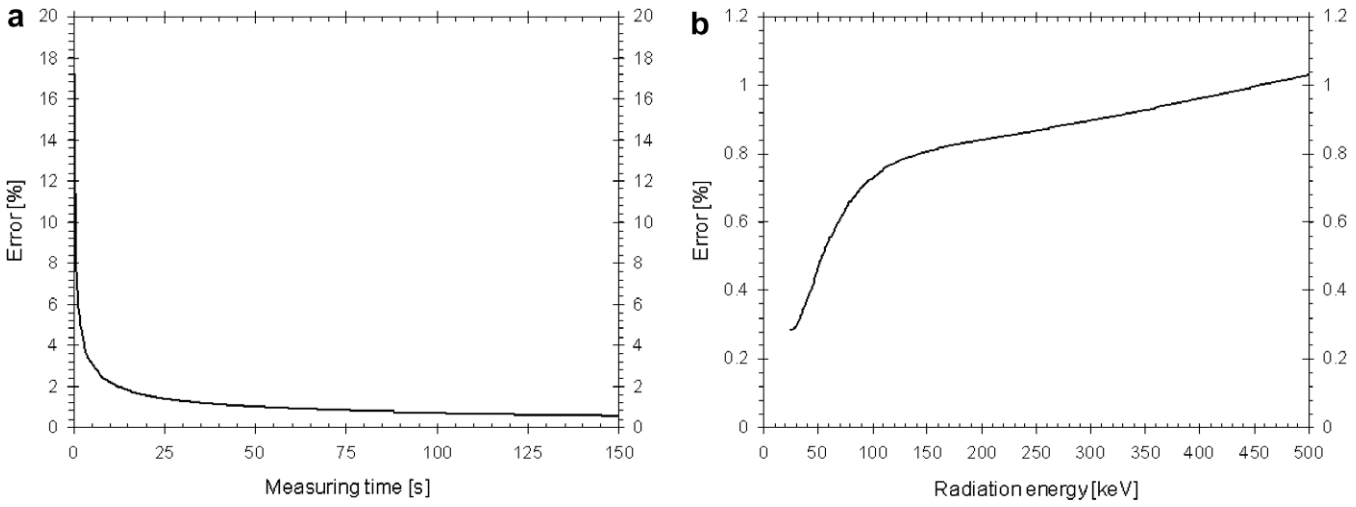

Fig. 13. Errors of gamma densitometry measurements: (a) error as a function of the measuring time, (b) error as a function of the radiation energy.

The present system transmits a 3 mm wide, parallel beam from a collimated source to a collimated detector. The source and the detector system is then traversed span-wise across the pipe cross-section. As the gamma beam is traversed, different liquid and wall lengths are observed. Hence, the error at different beam positions in the same counting time will be different as suggested by Eq. (19). In order to study this effect, it is necessary to calculate the beam averaged wall and liquid lengths that the beam passes through. Consider a beam of thickness b passing through a circle of radius r_{int} at distance y from the center as illustrated in Fig. 14a. An average liquid length (H_{Liq}) across the thickness of the gamma beam can be calculated by dividing this area by the beam thickness b as given below (Watson, 1998):

$$H_{Liq} = \frac{r_{\text{int}}^2}{2b}[\sin(2\theta) + 2\theta]_{\arcsin\left(\frac{y'}{r_{\text{int}}}\right)}^{\arcsin\left(\frac{y'+b}{r_{\text{int}}}\right)} \tag{21}$$

where θ is in radians as indicated in Fig. 14a. Similarly, the averaged wall length (H_{wall}) can be estimated as given below:

$$H_{\text{wall}} = \frac{r_{ext}^2}{2b}[\sin(2\theta) + 2\theta]_{\arcsin\left(\frac{y'}{r_{ext}}\right)}^{\arcsin\left(\frac{y'+b}{r_{ext}}\right)} - \frac{r_{\text{int}}^2}{2b}[\sin(2\theta) + 2\theta]_{\arcsin\left(\frac{y'}{r_{\text{int}}}\right)}^{\arcsin\left(\frac{y'+b}{r_{\text{int}}}\right)} \tag{22}$$

where r_{ext} represents the external radius of the pipe. The total distance (H), can be calculated as:

$$H = H_{Liq} + H_{\text{wall}} \tag{23}$$

Eqs. (19), (21), (22), and (23) can be used to estimate the measurement error as a function of the distance from the center of the pipe to the gamma beam as illustrated in Fig. 14b. In this case, following assumptions are made: constant incident gamma beam intensity (I_0 = 28,400 counts/s), measuring time (t = 50 s), phase fraction (ε_w = 1) and constant linear attenuation coefficients for fluids and wall. The largest error is observed when the gamma beam in located very close to the pipe wall. The error decreases as the gamma beam moves towards the center of the pipe. The minimum error of 0.53% is observed at the center of the pipe. While measuring close to the pipe wall, parts of the gamma beams hit the wall instead of the flow, making the control volume very small. The accuracy of the gamma densitometer decreases with decreasing control volume, thus severely reduced accuracy is expected in the measurements closest to the pipe wall.

5. Conclusions

Single-beam gamma densitometry is a non-intrusive, reliable and relatively inexpensive method of component fraction mea-

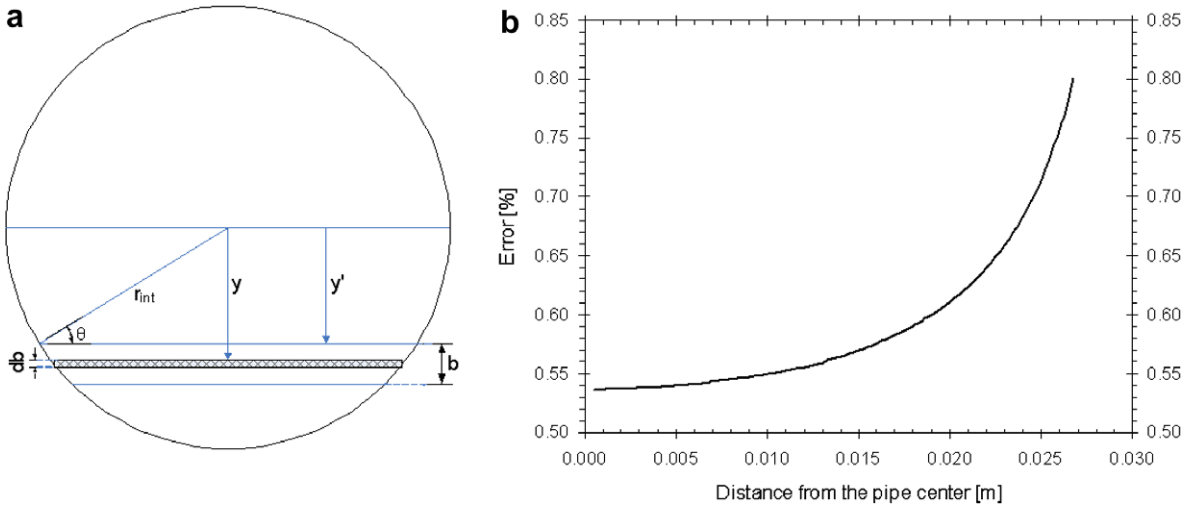

Fig. 14. Measurement error due to different beam position: (a) calculation of averaged liquid thickness, (b) error as a function of beam position.

surements in multiphase flow systems. In the present work, single-beam gamma densitometer is used to measure water volume fractions in oil–water flow in horizontal and slightly inclined pipes. The water hold-up, slip ratio and frictional pressure drop data are presented based on gamma densitometry measurements. The measurement uncertainties associated with single-beam gamma densitometry are also discussed.

In general, higher water hold-up values are observed for upwardly inclined pipes. For downwardly inclined pipes, lower water hold-up values are observed compared to the horizontal and upwardly inclined pipes. The measurements show that the water hold-up is very sensitive for pipe inclination at lower mixture velocities. For all pipe inclinations, at mixture velocities 0.25 and 0.50 m/s, the slip ratio decreases as water cut increases. As the mixture velocity increases the slip ratio approaches one, due to increased level of mixing. At higher mixture velocity, U_m = 1.00 m/s, there are marginal differences in hold-up and slip ratio measurements for horizontal and near horizontal flows. The water phase is dispersed in the oil at higher mixture velocities for lower inlet water cuts giving smaller slip ratios. In general, the present observations on water hold-up and slip ratio show a good consensus with previous investigations.

The frictional pressure drop is estimated based on measured total pressure drop and water hold-up data. At low mixture velocity, U_m = 0.25 m/s, there are smaller variations of frictional pressure drop with inlet water cut. A peak in pressure drop is observed at higher inlet water cuts at mixture velocities, 0.50 and 1.00 m/s. At these mixture velocities, the oil phase is dispersed in the water. The observed peak in frictional pressure drop can be attributed to the dispersion effect of oil in the water phase. The measured frictional pressure drop profiles for horizontal and inclined flows show some similarities in their overall shape. The frictional pressure drop in upwardly inclined pipes is slightly higher than in horizontal pipes. This could be directly attributed to the increased turbulence level associated with wavy flow structure. However, marginal differences in frictional pressure drop are observed between horizontal and downwardly inclined flows.

The measurement uncertainties associated with single-beam gamma densitometer are also discussed. The statistical error is mainly governed by the measuring time, radiation energy and the beam position for a given system. Time duration of 50 s is used as the measuring time at each point giving an acceptable error of 0.97%. Higher accuracy can be achieved by increasing the measuring time. The radiation energy of 59.5 keV from Am-241 source gives an error about 0.54%. The measurement error strongly depends on the beam position. The large measurement errors are observed when the beam is close to the pipe wall. The minimum error of 0.53% is observed at the center of the pipe. From the results presented, it can be concluded that the single-beam gamma densitometer can be successfully used to measure phase fractions in oil–water flow systems with an acceptable accuracy.

References

Abduvayt, P., Manabe, R., Watanabe, T., Arihara, N., 2004. Analysis of oil–water flow tests in horizontal, hilly-terrain and vertical pipes. In: Proc. Annual SPE Tech. Conf., Houston, Texas (SPE 90096), in CD ROM.

Åbro, E., Johansen, G.A., 1998. Improved void fraction determination by means of multibeam gamma-ray attenuation measurements. Flow Meas. Instrum. 10, 99–108.

Alkaya, B., 2000. Oil–water flow patterns and pressure gradients in slightly inclined pipes. M.S. Thesis, University of Texas, Austin, USA.

Angeli, P., Hewitt, G.F., 1998. Pressure gradient in horizontal liquid–liquid flows. Int. J. Multiphase Flow 24, 1183–1203.

Blaney, S., Yeung, H., 2007. Investigation of the exploitation of a fast-sampling gamma densitometer and pattern recognition to resolve the superficial phase velocities and liquid phase water cut of vertically upward multiphase flows. Flow Meas. Instrum. 19, 57–66.

Brennen, C.E., 2005. Fundamentals of Multiphase Flows. Cambridge University Press. ISBN 052184804.

Bukur, D.B., Daly, J.G., Patel, S.A., 1996. Application of γ-ray attenuation for measurement of gas hold-ups and flow regime transition in bubble columns. Ind. Eng. Chem. Res. 35, 70–80.

Chan, A.M.C., Banerjee, S., 1981. Design aspects of gamma densitometers for void fraction measurements in small-scale two-phase flows. Nucl. Instrum. Methods 190, 135–148.

Chaouki, J., Larachi, F., Duduković, M., 1997. Non-invasive Monitoring of Multiphase Flows. Elsevier, Amsterdam.

Cox, A.L., 1985. A study of horizontal and downhill two-phase oil–water flow. M.S. Thesis, University of Tulsa.

Eberle, C.S., Leung, W.H., Ishi, M., Kevanker, S.T., 1994. Optimization of a one-shot gamma densitometer to measuring area-averaged void-fractions of gas–liquid flows in narrow pipe. Meas. Sci. Technol. 5, 1146–1158.

Elseth, G., 2001. An experimental study of oil–water flow in horizontal pipes. PhD Thesis, Telemark University College, Porsgrunn.

Fano, U., 1953. Nucleonics 11 (8), 8–12.

Flores, J.G., Sarica, C., Chen, X.T., Brill, J.P., 1998. Investigation of holdup and pressure drop behavior for oil–water flow in vertical and deviated wells. Trans. ASME J. Energy Resour. Technol. 120, 8–14.

Grodstein, G.W., 1957. X-ray attenuation coefficients from 10 keV to 100 MeV. NBS Circular 583.

Hewitt, G.F., 1978. Measurement of two-phase flow, New York.

Jiang, Y., Rezkallah, K.S., 1993. An experimental study of the suitability of using a gamma densitometer for void fraction measurements in gas–liquid flow in a small diameter tube. Meas. Sci. Technol. 4, 496–505.

Kok, H.V., Van der Hagen, T.H.J.J., Mudde, R.F., 2001. Subchannel void-fraction measurements in a 6×6 rod bundle using a simple gamma-transmission method. Int. J. Multiphase Flow 27, 147–170.

Kumara, W.A.S., Halvorsen, B.M., Melaaen, M.C., 2009a. Pressure drop, flow pattern and local water volume fraction measurements of oil–water flow in pipes. Meas. Sci. Technol. 20, 114004 (18pp).

Kumara, W.A.S., Halvorsen, B.M., Melaaen, M.C., 2009b. Velocity and turbulence measurements of oil–water flow in horizontal and slightly inclined pipes using PIV. Computational Methods in Multiphase Flow V. WIT Press. pp. 277–292.

Lum, J.Y.L., Lovick, J., Angeli, P., 2002. Two-phase liquid flows in inclined pipelines. In: Proc. 3rd North American Conference on Multiphase Flow.

Lum, J.Y.L., Lovick, J., Angeli, P., 2004. Low inclination oil–water flows. Can. J. Chem. Eng. 82, 303–315.

Lum, J.Y.L., Al-Wahaibi, T., Angeli, P., 2006. Upward and downward inclination oil–water flows. Int. J. Multiphase Flow 32, 413–435.

Moffat, R.J., 1988. Describing uncertainties in experimental results. Exp. Therm. Fluid Sci. 1, 3–17.

Müller, J.W., 1973. Dead time problems. Nucl. Instrum. Methods 112, 47–57.

Nädler, M., Mewes, D., 1997. Flow induced emulsification in the flow of two immiscible liquids in horizontal pipes. Int. J. Multiphase Flow 23, 55–68.

Pan, L., 1996. Pressure three-phase (gas–liquid–liquid) flows. PhD Thesis, Imperial College, London.

Petrick, M., Swanson, B.S., 1958. Radiation attenuation method of measuring density of a two-phase fluid. Rev. Sci. Instrum. 29, 1079–1085.

Prasser, H.-M., 2008. Novel experimental measuring techniques required to provide data for CFD validation. Nucl. Eng. Des. 238, 744–770.

Prasser, H.-M., Böttger, A., Zschau, J., 1998. A new electrode-mesh tomograph for gas–liquid flows. Flow Meas. Instrum. 9, 111–119.

Reda, D.C., Hadley, G.R., Turner, J.E.R., 1981. Application of the gamma-beam attenuation technique to the measurement of liquid saturation for two-phase flows in porous media. Instrumentation in the Aerospace Industry, vol. 27. In: Kissell, K.E., (Ed.), Advances in Test Measurement, Part 2, Proceedings of the 27th International Instrumentation Symposium, vol. 18, Instrument Society of America, Research Triangle Park, NC, pp. 553–568.

Rodriguez, O.M.H., Oliemans, R.V.A., 2006. Experimental study on oil–water flow in horizontal and slightly inclined pipes. Int. J. Multiphase Flow 32, 323–343.

Schlieper, G., Huppmann, W.J., Kozuch, A., 1987. Non-destructive determination of sectional densities by the gamma densomat. Prog. Powder Metall. 43, 351–362.

Scott, G.M., 1985. A study of two-phase liquid–liquid flow at variable inclinations. M.S. Thesis, University of Texas at Austin, USA.

Spindler, K., Löffel, R., Hahne, E., 1988. Gamma densitometer for void fraction measurements in two-phase flows. Tech. Mess. 55 (6), 228–233.

Sprowll, R.L., Phillips, W.A., 1980. Modern Physics: The Quantum Physics of Atoms, Solids and Nuclei, third ed. Wiley, New York.

Stahl, P., Rohr, P.R.V., 2004. On the accuracy of void fraction measurements by single beam gamma-densitometry for gas–liquid two-phase flows in pipes. Exp. Therm. Fluid Sci. 28, 533–544.

Thorn, R., Johansen, G.A., Hammer, E.A., 1997. Recent developments in three-phase flow measurement. Meas. Sci. Technol. 8, 691–701.

Tjugum, S.A., Frieling, J., Johansen, G.A., 2002. A compact low energy multibeam gamma-ray densitometer for pipe-flow measurements. Nucl. Instrum. Methods Phys. Res., B 197, 301–309.

Valle, A., Utvik, O.H., 1997. Pressure drop, flow pattern and slip for two-phase crude oil-water flow: experiments and model predictions. In: Proc. International Symposium on Liquid-liquid Two-phase Flow and Transport Phenomena, Antalya, Turkey.

Watson, M.J., 1998. Report on the commissioning of the Norsk hydro traversing gamma densitometer for liquid–liquid experiments. Internal Report, Norsk Hydro Research Centre, Porsgrunn, Norway.